Available online at www.sciencedirect.com

ScienceDirect

Ceramics International 40 (2014) 4135–4140

CERAMICS INTERNATIONAL

www.elsevier.com/locate/ceramint

Ceramic/metal nanocomposites by lyophilization: Spark plasma sintering and hardness

C.F. Gutierrez-Gonzalez[a], S. Agouram[b], R. Torrecillas[a,c], J.S. Moya[d], S. Lopez-Esteban[d,*]

[a]Centro de Investigación en Nanomateriales y Nanotecnología (CINN), Consejo Superior de Investigaciones Científicas (CSIC), Universidad de Oviedo (UO), Principado de Asturias (PA), Parque Tecnológico de Asturias, 33428 Llanera, Spain
[b]Department of Applied Physics and Electromagnetism, Universitat de Valencia, 46100 Burjassot, Spain
[c]Moscow State University of Technology "STANKIN", Vadkovskij per. 1, Moscow Oblast, Moscow, Russian Federation
[d]Instituto de Ciencia de Materiales de Madrid (ICMM), Consejo Superior de Investigaciones Cientificas (CSIC), Cantoblanco, 28049 Madrid, Spain

Received 3 July 2013; received in revised form 15 August 2013; accepted 15 August 2013
Available online 2 September 2013

Abstract

The present study is focused on the procedure of spray-drying and lyophilization techniques for the preparation of ceramic/metal nanocomposites. The results of the study at all stages are compared with those corresponding to powders conventionally dried by heating in furnace. Starting from aqueous solutions of metal salts and ceramic powders, the procedure follows with spray-drying, lyophilization, calcination of the resulting powders and subsequent Spark Plasma Sintering (SPS). X-ray diffraction analysis of the powders at different stages of the processing routes was used for phase indexing; further characterization was performed by Transmission Electron Microscopy and Energy Dispersive X-Ray Spectroscopy, revealing that the sizes of the metal particles obtained are in the nanometer range and appear homogeneously and well dispersed on the zirconia surface. The mechanical performance of the SPSed compacts was studied by means of the Vickers hardness, showing excellent results: an increase of 30% with respect to pure zirconia.

Keywords: B. Nanocomposites; C. Hardness; C. Mechanical properties; D. ZrO_2; Freeze-drying

1. Introduction

The synthesis of metal nanoparticles has acknowledged significant consideration in the last years due to potential applications for their unusual properties related to magnetism, optics, electronics, catalysis, hardness, etc. [1–4]. More specifically, nickel nanoparticles find important applications in magnetic, conducting, catalyst materials, wear resistance, etc. [5–8]. There are crucial difficulties in dealing with the manipulation of nanoparticles: (i) many of the applications of metal nanoparticles are size dependent [9] and, thus, control of the nanoparticle size is essential. (ii) The high surface energy of these particles makes them extremely reactive and most nanoparticles undergo aggregation without protection or passivation of their surfaces; a good dispersion is crucial to reach exceptional properties. (iii) Moreover, for certain specific metals among which is nickel, the synthesis of pure metal nanoparticles is relatively difficult because they are easily oxidized. A successful approach to avoid all these problems is to keep the metal nanoparticles embedded in a ceramic matrix, in the so-called ceramic/metal composite materials ("cermets"). Cermets have involved noteworthy consideration because of an extraordinary combination of properties that makes them excellent aspirants for the production of multifunctional devices. Moreover, the fact that one of the phases is nanostructured, substantially modifies the mechanical, electrical, magnetoresistive, and magnetic properties of the composite [10].

Different preparation processes of ceramic–metal nanocomposite powder can be found in the literature [1,10–12], each of them leading to different microstructures and, hence, a wide range of properties. Thin-film deposition methods produce nice monodisperse nanoparticles but generally small amounts of sample; on the other hand, volumetric procedures allow larger amounts of sample, but nanoparticles appear mostly agglomerated. A homogeneous dispersion of particles into the matrix is crucial to the behavior of cermets, especially in the field of

*Corresponding author. Tel.: +34 91 334 90 00; fax: +34 91 372 06 23.
E-mail address: s.lopez.esteban@csic.es (S. Lopez-Esteban).

0272-8842/$ - see front matter © 2013 Elsevier Ltd and Techna Group S.r.l. All rights reserved.
http://dx.doi.org/10.1016/j.ceramint.2013.08.068

functional applications. As mentioned above regarding the metals, the synthesis of nanoparticles is not the main problem, but their manipulation in order to avoid the presence of large aggregates.

Nowadays, spray-drying and lyophilization (also known as "freeze-drying") are techniques considered as an alternative route for ceramic powder preparations [13–15]: (i) On one hand, spray-drying consists of the direct vaporization of the precursor solution and drying of the droplets while they are in free fall. It allows dividing the suspension into very small drops, which increases the speed of freezing when sprayed over liquid nitrogen. This procedure avoids the segregation of components and results in homogeneous uniform spherical particles. (ii) On the other hand, lyophilization consists of sublimating ice under vacuum and low temperature conditions. When the lyophilization is properly controlled, water separates from the solid phases by sublimation. It has been demonstrated as a very suitable method to eliminate the capillary forces which are the origin of agglomeration of the nanoparticles. Therefore, it allows obtaining uniform powders by preventing drying agglomerates [16].

More specifically, it has been explained in previous works the potential of the spraying-lyophilization technique for composite materials [12]. These works have demonstrated that combining spray-freezing with lyophilization is a feasible technique for preparing ceramic/metal nanostructured powders. In this work, three different metal contents in the zirconia/nickel system have been studied, showing in all cases that the resulting powders present accurate composition, homogeneity, good dispersion of metal and apparent crystallinity. The metal nanoparticles have grown epitaxially on the ceramic surface giving rise to good interfaces, which is crucial to obtain excellent mechanical properties in the corresponding sintered materials.

Following this set of results, the aim of the present work is to study the physical features, microstructure and mechanical properties of the zirconia/nickel nanocomposites obtained by Spark Plasma Sintering (SPS) starting from spray-dried and lyophilized powders. Likewise, the results are compared with those corresponding to nanopowders dried conventionally by heating.

2. Materials and methods

The following commercially available powders have been used as raw materials: (1) Tetragonal zirconia polycrystals (3Y–TZP, 3 mol% Y_2O_3; TZ–3YE, *Tosoh Corp.*), with an average particle size of $d_{50}=0.26\pm0.05$ μm; (2) nickel (II) nitrate hexahydrate (*Merck*, Germany, 99.0% purity, Ni $(NO_3)_2\cdot 6H_2O$). Nickel nitrate salt powders were dispersed in distilled water by ultrasonic agitation in a suitable volume to achieve total dilution. The ceramic powder was added in order to obtain zirconia/Ni composites with a metal content of 1 vol% Ni, 2.5 vol% Ni and 3.5 vol% Ni. The suspensions were milled for 24 h with zirconia balls in order to get homogeneous slurries.

Two drying methods were used to compare the properties of the final composites: (A) by heating in a conventional furnace, according to the method reported elsewhere [10] (samples denoted as "T1.0", "T2.5" and "T3.5", respectively), and (B) by spray-freezing and freeze-drying according to the method reported by the Authors elsewhere [12] (samples denoted as: "LF1.0", "LF2.5" and "LF3.5", respectively). Pure zirconia has been processed by both methods for comparison purposes (denoted as "T0.0" and "LF0.0", respectively).

The resulting powders in both methods were calcined at 600 °C for 2 h in air to obtain ZrO_2/NiO powders. Finally, the metal oxide was reduced to metallic nickel in a 90%Ar/10%H_2 atmosphere at 500 °C for 2 h, obtaining a zirconia powder with metal nanoparticles adhered to the surface of the ceramic grains (zirconia/nNi). Subsequently, the different powders were spark plasma sintered (SPS, *FCT Systeme GMBH*, HPD 25, Germany) under the conditions 1350 °C, 25 kN, 5 min in hydrogen atmosphere.

An initial set of experiments was performed to characterize the powders obtained. The density of the powders was determined by using a Helium Pycnometer (*AccuPyc 1330*, *Micromeritics France S.A.*). X-ray diffraction analysis of the powders at different stages of the different processing routes was used for phase identification using CuK_α radiation (*XRD Bruker AXS D8 ADVANCE*, with a *SolX* energy-dispersive detector). Further characterization was performed by Transmission Electron Microscopy (TEM) by using a Field Emission Gun microscope (FEG) *TECNAI G2 F20* operating at 200 kV, and Energy Dispersive X-Ray Spectroscopy for EDX-mapping and quantitative TEM-EDX.

Regarding the SPS compacts, the density was measured according to the Archimedes method. The hardness was measured on 30 samples for each group (in terms of composition and drying method) in a Vickers diamond microindenter (*Leco 100-A* Microindentation Hardness Testing System, USA) on surfaces of cross sections polished down to 1 μm, with an applied load of 0.9 kg (8.8 N) for 15 s. The hardness was determined according to the equation $H_V=1.853\,P/d^2$, where P stands for the applied load (in N) and d stands for the diagonal length of the indentation (in mm). Pure zirconia was studied as control. The fracture surfaces were studied in a Field Emission Scanning Electron Microscope (FE-SEM, *Quanta FEG 650*, FEI), with Energy Dispersive X-ray Microanalysis (*Ametek*-EDX, with an *Apollo X* detector).

3. Results

Fig. 1 shows the X-ray diffractograms of samples with 3.5 vol% Ni obtained by both drying methods in study (samples LF3.5 and T3.5) in the range 10–70°. They have been recorded at different stages of the processing route, on powders as well as on samples sintered by SPS.

3.1. Powders: density and morphology. Average size of Ni nanoparticles

For all metal concentrations, the densities of the powders obtained by freeze-drying and by heating in furnace are shown in Table 1. Representative TEM micrographs and EDX-mapping of distributions of Ni nanoparticles and zirconia particles for the

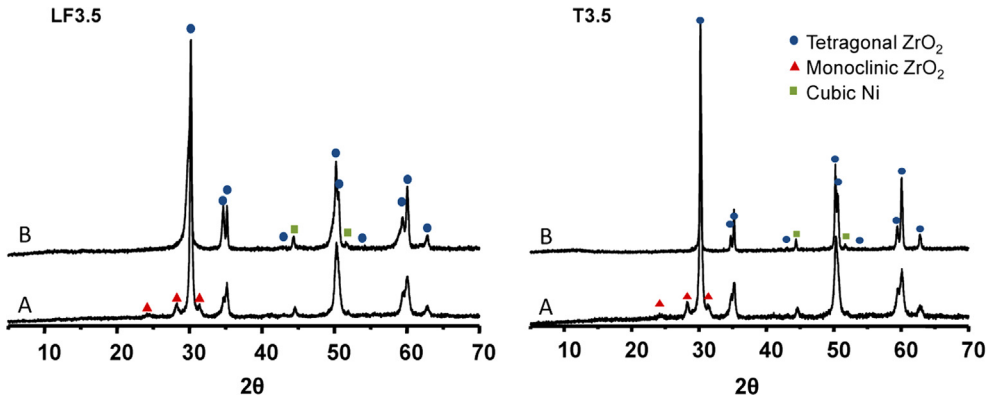

Fig. 1. X-Ray diffractograms corresponding to samples LF3.5 and T3.5, for (A) powders and (B) SPS sintered materials.

Table 1
Density of the different ceramic/metal powders determined with an helium pycnometer.

Sample	Density (g/cm^3)	Sample	Density (g/cm^3)
T1.0	5.9419 ± 0.0045	LF1.0	6.1057 ± 0.0042
T2.5	6.0168 ± 0.0020	LF2.5	6.2206 ± 0.0058
T3.5	5.9859 ± 0.0052	LF3.5	6.1774 ± 0.0042

different compositions are shown in Fig. 2. The mean size of the nickel nanoparticles in the powders obtained by both methods are shown in Fig. 3A. Table 2 shows the quantitative TEM-EDX analysis of the ceramic/metal powders obtained by both methods.

3.2. Sintered materials: density, average size of Ni nanoparticles, fracture surface, Vickers hardness

In the case of the sintered materials, the density was determined by the Archimedes principle (Table 3). The mean size of the nickel nanoparticles in the sintered materials is shown in Fig. 3B. Fig. 4 shows the SEM micrographs relative to the fracture surface of two samples with the same metal content (2.5 vol% Ni) obtained by both methods. The study of the Vickers hardness for samples obtained by both methods and all metal contents are presented in Fig. 5.

4. Discussion

The results obtained by X-Ray diffraction confirm that products at the first stage consisted only of zirconia (tetragonal and monoclinic) and nickel, with no presence of any other phases (Fig. 1, diffractogram A for both drying methods). After sintering, all samples consisted only of tetragonal-ZrO_2/*n*Ni (Fig. 1, diffractogram B for both drying methods). The same results were observed for the other two metal contents (1 vol% Ni and 2.5 vol% Ni). These results were supplemented by the quantitative TEM-EDX analysis (Table 2).

For all metal concentrations, the density of the powders obtained by freeze-drying was found to be higher than that of powders dried in furnace (Table 1). In the case of the sintered materials, it was found that those samples obtained after powders freeze-dried reached a density higher than those obtained following the route by heating in furnace (Table 3). These results are in accordance with the Ni mean sizes measured in the powders (Fig. 3A) in such a way that, the lower the Ni size in the powder, the higher the density of the sintered materials. The mean size of the nickel nanoparticles increases with the Ni content in the powders obtained by both methods (Fig. 3A). Both techniques allow obtaining nanoparticles with similar sizes for the lowest metal contents, increasing the differences with the Ni content. In all cases, the average size obtained by the lyophilization technique is lower than that obtained by heating in furnace. Representative TEM micrographs and EDX-mapping of distributions of Ni nanoparticles and zirconia particles for the different compositions (Fig. 2) reveal that the sizes of the metal particles obtained are in the nanometer range and appear homogeneously and well dispersed on the zirconia surface. Meanwhile, in the samples obtained by both methods, the fracture surfaces presented similar microstructures (Fig. 4).

The Spark Plasma Sintering technique was chosen as it is a relatively novel technique that makes possible to obtain dense nanocomposites having the nanostructured features of the ceramic/metal mixed powder previously processed. Moreover, it provides many advantages since very rapid sintering slopes can be achieved, giving uniform densities in the final compact with the addition of less additives as well as quite easy handling and low processing costs. In the case of sintered materials, around 150 particles from all over each sample were measured on fracture surfaces to determine the Ni particle size distribution for each composition. As indicated in Fig. 3B, the mean size of the nickel nanoparticles increases with the Ni content. In sample LF1.0 the particle size distribution is narrow and centered around 100 nm. Samples LF2.5 and LF3.5 present a distribution centered on bigger sizes, around 130 nm and 165 nm, respectively. The reason for this increment is due to the fact that, when increasing the Ni content, it is easier for the nanoparticles to coalesce. Even though the trend is the same for samples obtained by heating, the average size is slightly lower when processed by the lyophilization technique.

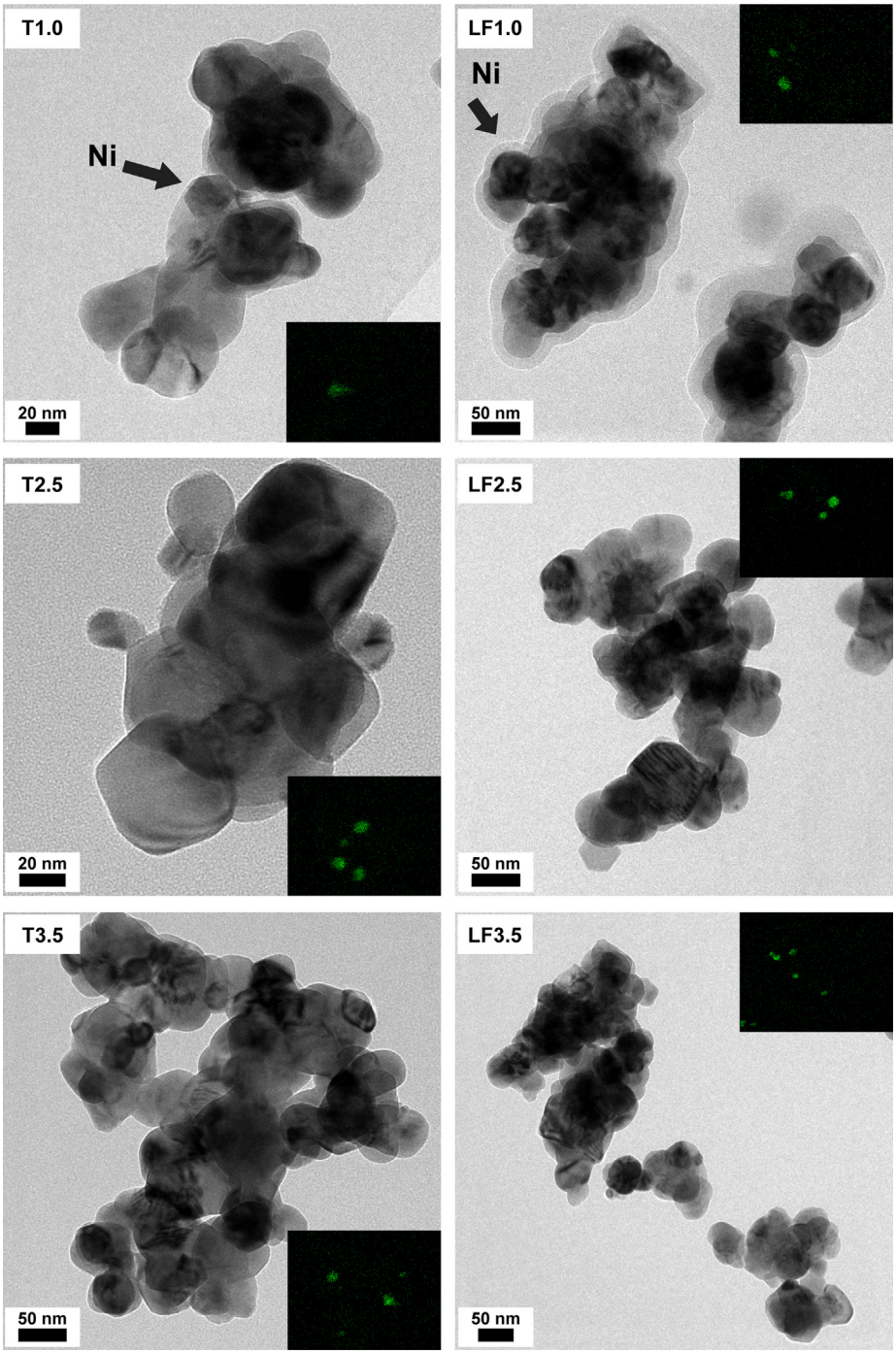

Fig. 2. TEM micrographs of the 3Y–TZP/Ni powders with the three different Ni contents studied (A). EDX mapping showing in either green or pink color the Ni nanoparticles (B). The Ni particles labeled have been identified by using all the EDX mapping availables (Ni, Zr and O). (For interpretation of the references to color in this figure legend, the reader is referred to the web version of the article).

As expected by taking into account other works [1,9,10,12], the presence of Ni nanoparticles increases the hardness respect to the value of pure zirconia. For both methods, the mechanical performance of the materials is excellent. The highest increase is 30% with respect to the hardness of pure zirconia, and corresponds to the composites with a metal content of 1 vol% Ni. There is no contradiction of these results with those presented elsewhere, where the maximum was found for samples with 2,5 vol% Ni, because in the present study the range of composition is much more narrow and, therefore, easier to reach a more accurate result. The hardness of the sintered materials is similar for both methods, as the size of the Ni nanoparticles was similar in the original composite powders.

Likewise, it has been studied elsewhere that, in all cases, the resulting powders presented accurate composition, homogeneity and good dispersion of metal nanoparticles and, moreover, the

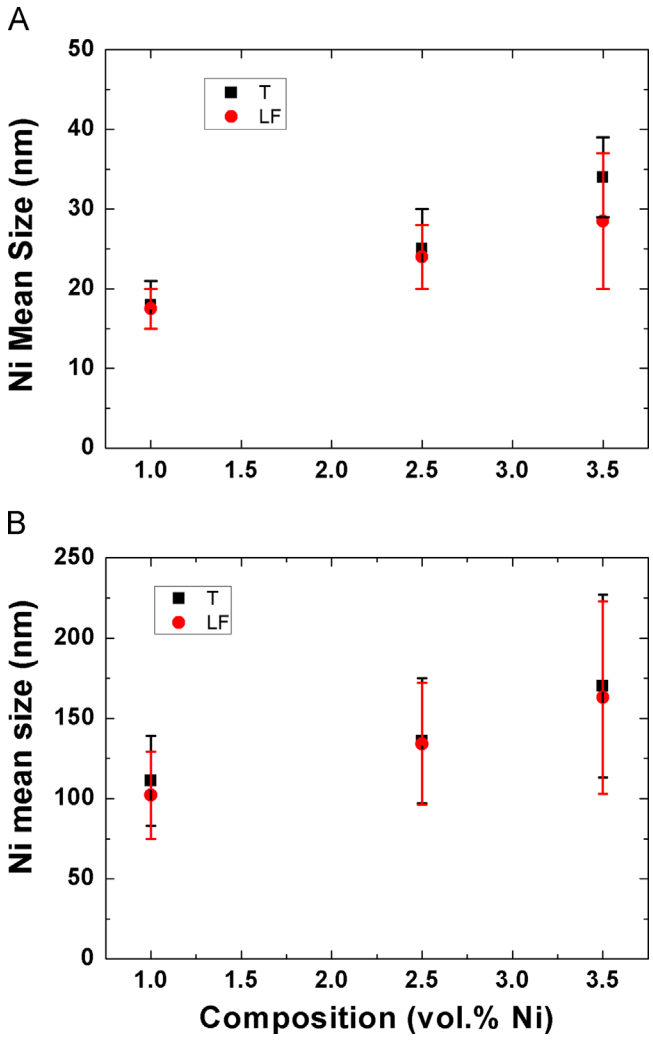

Fig. 3. Average size of Ni nanoparticles as a function of the initial Ni content (A) in the powders and (B) in the sintered nanocomposites.

Table 2
Quantitative TEM-EDX analysis of the ceramic/metal powders obtained by both methods (% at).

Sample	O	Zr	Ni	Sample	O	Zr	Ni
T1.0	67.7	31.5	0.8	LF1.0	69.4	29.0	1.6
T2.5	70.0	27.7	2.3	LF2.5	69.2	28.2	2.6
T3.5	67.0	30.2	2.8	LF3.5	65.8	31.0	3.2

interfaces are ordered, neat, showing that the Ni crystals have grown epitaxially on the surface of zirconia submicron grains. The present work proves that this potentially positive feature truly leads to excellent mechanical properties of the corresponding sintered materials, very similar for both methods. This means that the key of the formation of the nickel nanoparticles was only in the preparation of the aqueous ceramic/metal suspensions, and not in the way of drying. In the suspensions, the formation of the nanoparticles consists in the precipitation of a large population of Ni_2^+ ions on the surface of the zirconia particles through O–H bridges (as the presence of $Ni(OH)_2$ has been demonstrated by infrared measurements), and subsequent epitaxial growth of the metal nanoparticles, as well reported in [10]. Indeed, the nucleation process of nanoparticles on the surface of the ceramic particles can prevent the growth of the

Table 3
Density of the different ceramic/metal Spark Plasma Sintered materials determined by the Archimedes principle.

Sample	% Density ($\pm$0.1)	Sample	% Density ($\pm$0.1)
T1.0	98.9	LF1.0	99.7
T2.5	99.1	LF2.5	> 99.9
T3.5	99.5	LF3.5	99.9

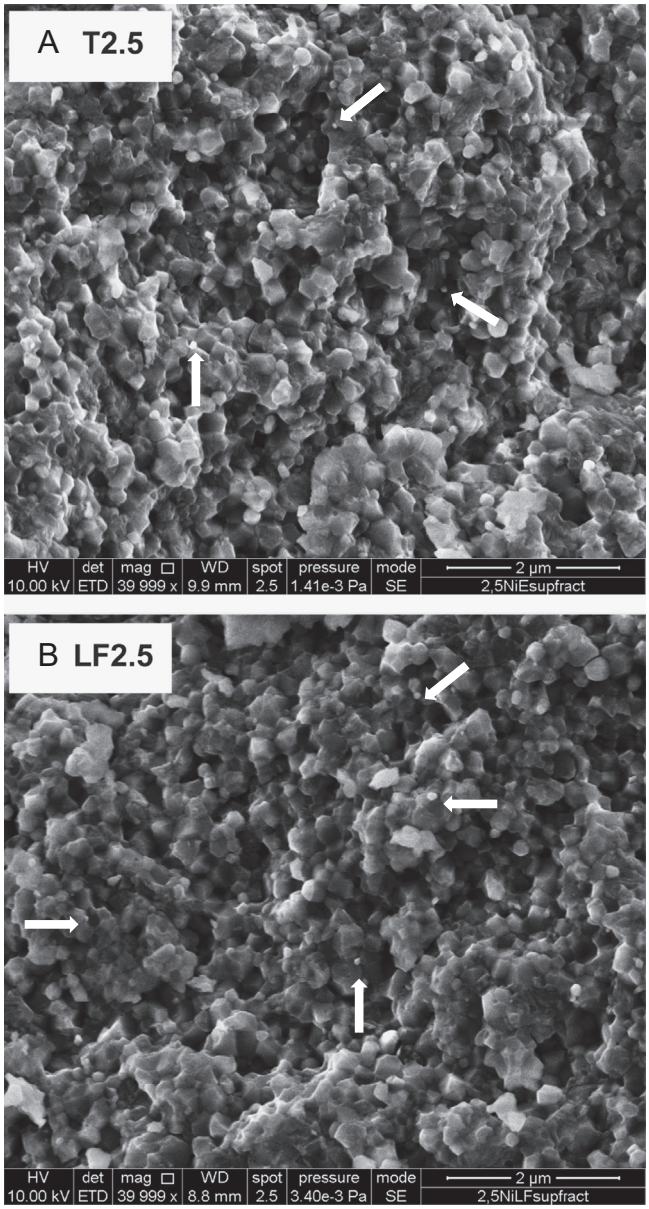

Fig. 4. FE-SEM images of the fracture surfaces of samples with 2.5 vol% Ni sintered by SPS by both methods: dried in furnace (A) and lyophilized (B). Arrows point at some randomly chosen nickel nanoparticles identified by EDX.

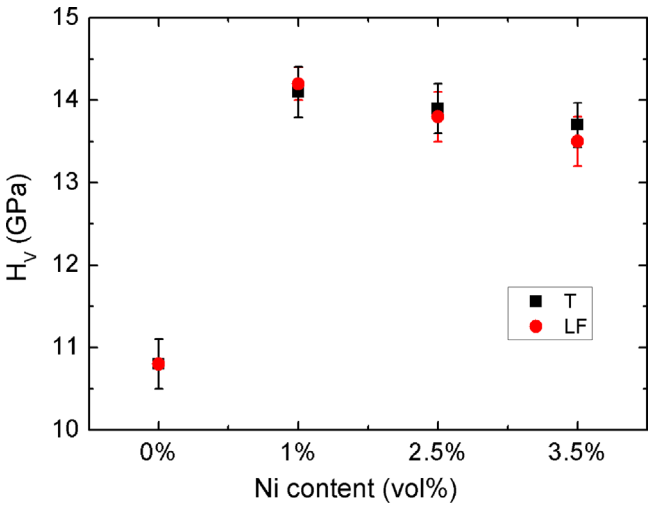

Fig. 5. Vickers hardness of ZrO_2/Ni nanocomposites obtained by both methods, for increasing volume contents of Ni. The value corresponding to pure zirconia has been plotted for comparison purposes.

nanoparticles and, therefore, the nanocomposite properties can be improved. Besides, this simple method allows large amounts of sample to be obtained. These results make this wet-processing route very reliable in order to fabricate ceramic/metal advanced nanocomposites.

This work demonstrates that spray-freezing combined with freeze-drying are feasible techniques to fabricate reliable ceramic/metal nanostructured powders that lead to compacts with excellent nanostructures and mechanical features.

5. Conclusions

For all metal concentrations, the density of the powders obtained by spray-drying and lyophilization was found to be higher than that of powders dried in furnace; the corresponding sintered materials followed the same trend. The average mean size of the nickel nanoparticles in the powders obtained by the lyophilization technique is slightly lower than that obtained by heating in furnace; in the compacts, the divergence is negligible. The metal particles obtained are in the nanometer range and appear homogeneously and well dispersed on the zirconia surface. For both methods, the mechanical performance of the materials is excellent. The Vickers hardness increases up to 30% with respect to the hardness of pure zirconia.

Acknowledgments

This work was supported by the Spanish Ministry of Science and Innovation (MICINN) under the Project MAT2009-14542-C02, by the Spanish Ministry of Economy and Competitiveness (MINECO) under the Project MAT2012-38645, and the Government of the Principality of Asturias through PCTI and ERDF (European Regional Development Fund) 2007–2013 under Project PC10-65. The Authors are grateful to the Central Support Service in Experimental Research (SCSIE), University of Valencia (Spain) for providing access to the TEM facility. C.F. Gutierrez-Gonzalez acknowledges CSIC and ESF for the concession of a JAE-Doc 2009 grant. Thanks to the Ministry of Education and Science of the Russian Federation in the frame of Governmental Regulation of the Russian Federation N220, 9th of April 2010.

References

[1] J.S. Moya, S. Lopez-Esteban, C. Pecharroman, The challenge of ceramic/metal microcomposites and nanocomposites, Progress in Materials Science 52 (2007) 1017–1090.
[2] Y. Sun, Y. Xia, Shape-controlled synthesis of gold and silver nanoparticles, Science 298–5601 (2002) 2176–2179.
[3] K.L. Kelly, E. Coronado, L.L. Zhao, G.C. Schatz, The optical properties of metal nanoparticles: The influence of size, shape, and dielectric environment, Journal of Physical Chemistry B 107 (2003) 668–677.
[4] C. Burda, X. Chen, R. Narayanan, M.A. El-Sayed, Chemistry and properties of nanocrystals of different shapes, Chemical Review 105 (2005) 1025–1102.
[5] H.H. Delavari, H.R. Madaah Hosseini, M. Wolff, Modeling of self-controlling hyperthermia based on nickel alloy ferrofluids: proposition of new nanoparticles, Journal of Magnetism and Magnetic Materials 335 (2013) 59–63.
[6] J. Park, E. Kang, S.U. Son, et al., Monodisperse nanoparticles of Ni and NiO: synthesis, characterization, self-assembled superlattices, and catalytic applications in the suzuki coupling reaction, Advanced Materials 17 (2005) 429–434.
[7] K.-I. Shimizu, K. Kon, K. Shimura, S.S.M.A. Hakim, Acceptor-free dehydrogenation of secondary alcohols by heterogeneous cooperative catalysis between Ni nanoparticles and acid–base sites of alumina supports, Journal of Catalysis 300 (2013) 242–250.
[8] T. Rodriguez-Suarez, J.F. Bartolomé, A. Smirnov, S. Lopez-Esteban, R. Torrecillas, J.S. Moya, Sliding wear behavior of alumina/nickel nanocomposites processed by a conventional sintering route, Journal of the European Ceramic Society 31 (2011) 1389–1395.
[9] S. Lopez-Esteban, T. Rodriguez-Suarez, F. Esteban-Betegon, C. Pecharroman, J.S. Moya, Mechanical properties and interfaces of zirconia/nickel in micro- and nanocomposites, Journal of Materials Science 41 (2006) 5194–5199.
[10] F. Esteban-Betegon, S. Lopez-Esteban, J. Requena, C. Pecharroman, J.S. Moya, J.C. Conesa, Obtaining Ni nanoparticles on 3Y-TZP powder from nickel salts, Journal of the American Ceramic Society 89 (2006) 144–150.
[11] E. Fernandez-Garcia, C.F. Gutierrez-Gonzalez, A. Fernandez, R. Torrecillas, S. Lopez-Esteban, Processing and spark plasma sintering of zirconia/titanium cermets, Ceramics International 39 (2013) 6931–6936.
[12] C.F. Gutierrez-Gonzalez, S. Agouram, R. Torrecillas, J.S. Moya, S. Lopez-Esteban, Ceramic/metal nanocomposites by lyophilization: processing and HRTEM study, Materials Research Bulletin 47 (2012) 285–289.
[13] Z.L. Wang, W.H. Finlay, M.S. Peppler, L.G. Sweeney, Powder formation by atmospheric spray-freeze-drying, Powder Technology 170 (2006) 45–52.
[14] A. Gurav, T. Kodas, T. Pluym, Y. Xiong, Aerosol processing of materials, Aerosol Science and Technology 19 (1991) 411–452.
[15] T. Stoyanova Lyubenova, F. Matteucci, A. Costa, M. Dondi, J. Carda, Ceramic pigments with sphene structure obtained by both spray- and freeze-drying techniques, Powder Technology 193 (2009) 1–5.
[16] A.G. King, Ceramic Technology and Processing, vol. 1, William Andrew Publishing, New York, USA, 2002 (pp. 136–142).